CHEMISTRY & SUSTAINABILITY

CHEMSUSCHEM

ENERGY & MATERIALS

Accepted Article

Title: Small current but large production of 1,3-propanediol from glycerol by an electrode-driven metabolic shift in Klebsiella pneumoniae L17

Authors: Changman Kim, Jae Hyeon Lee, Jiyun Baek, Da Seul Kong, Jeong-Geol Na, Jinwon Lee, Eric Sundstrom, Sunghoon Park, and Jung Rae Kim

To be cited as: *ChemSusChem* 10.1002/cssc.201902928

Link to VoR: http://dx.doi.org/10.1002/cssc.201902928

A Journal of

ChemPubSoc Europe

WILEY-VCH

www.chemsuschem.org

Date: December 06 2019

For resubmission to *ChemSusChem after revision* (Manuscript number: cssc.201902928)

Small current but large production of 1,3-propanediol from glycerol by an electrode-driven metabolic shift in *Klebsiella pneumoniae* L17

Changman Kim[1,†], Jae Hyeon Lee[1], Jiyun Baek[1], Da Seul Kong[1], Jeong-Geol Na[2], Jinwon Lee[2], Eric Sundstrom[3], Sunghoon Park[4], Jung Rae Kim[1,*]

[1] School of Chemical and Biomolecular Engineering, Pusan National University, Busan, 609-735, Republic of Korea.

[2] Department of Chemical and Biomolecular Engineering, Sogang University, 35 Baekbeom-Ro, Mapo-Gu, Seoul 04107, Republic of Korea

[3] Advanced Biofuel and Bioproducts Process Development Unit, Lawrence Berkeley National Laboratory, Emeryville, CA, 94608, USA

[4] School of Energy and Chemical Engineering, UNIST, Ulsan, 689-798, Republic of Korea

[†]Present Address: Advanced Biofuel and Bioproducts Process Development Unit, Lawrence Berkeley National Laboratory, Emeryville, CA, 94608, USA

Running title: Electro-fermentation of 1,3-PDO

[*]**Corresponding author**

Jung Rae Kim, PhD

Address: School of Chemical and Biomolecular Engineering,

Pusan National University, Busan 609-735, Republic of Korea

E-mail address: j.kim@pusan.ac.kr

Phone: +82.51.510.2393

Fax: +82.51.510.3943

Graphical Abstract

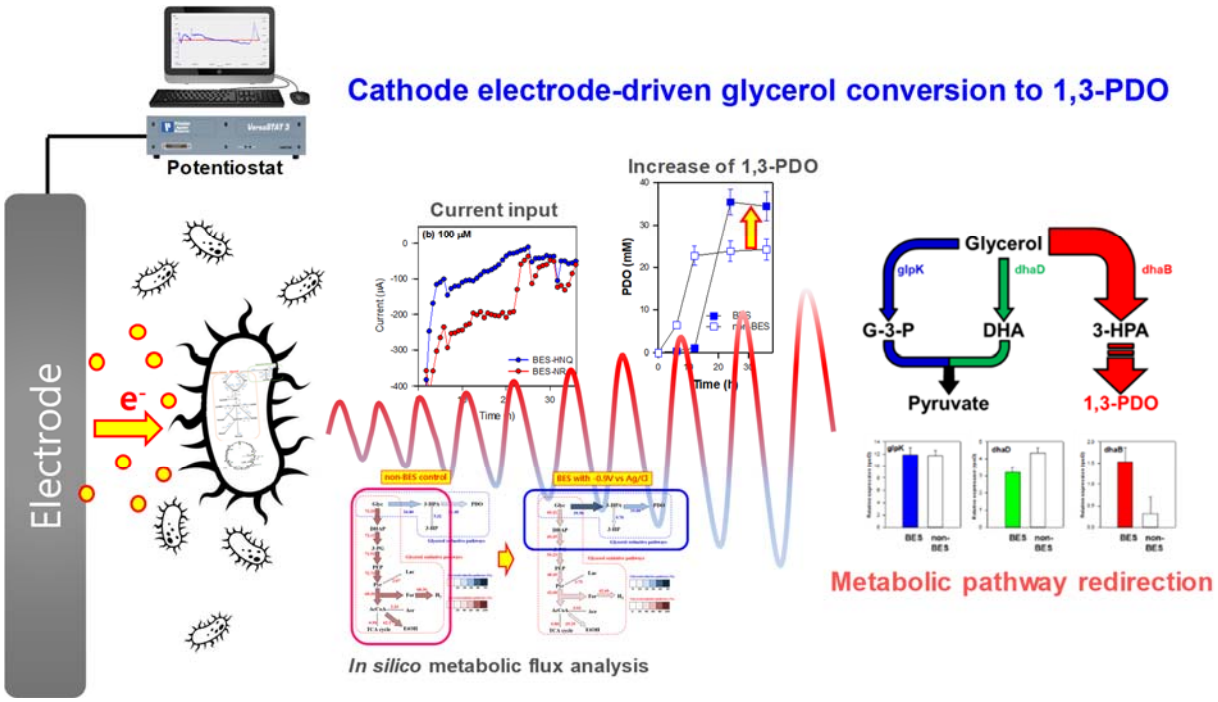

Abstract

Electro-fermentation actively regulates the bacterial redox state, which is essential for bioconversion, and has been highlighted for further improvements of the productivity of either reduced or oxidized platform chemicals. 1,3-Propanediol (1,3-PDO) is an industrial value-added chemical that can be produced from glycerol fermentation. The bioconversion of 1,3-PDO from glycerol requires additional reducing energy under anoxic conditions. This study examined the cathode electrode-based conversion of glycerol to 1,3-PDO with various electron shuttles (2-hydroxy-1,4-naphthoquinone, neutral red, and hydroquinone) using *Klebsiella pneumoniae* L17. The externally-poised potential of - 0.9 V vs. Ag/AgCl to the cathode electrode increased 1,3-PDO (35.5 ± 3.1 mM) production when 100 μM of neutral red was used compared to non-BES fermentation (23.7 ± 2.4 mM). Stoichiometric metabolic flux and transcriptional analysis indicated a shift in the carbon flux toward the glycerol reductive pathway. The homologous overexpression of DhaB and DhaT enzymes enhanced 1,3-PDO conversion (39.3 ± 0.8 mM) synergistically under cathode electrode-driven fermentation. Interestingly, small current uptake (0.23 mmol of electrons) caused significant metabolic flux changes with a concomitant increase in 1,3-PDO production. This suggests that both an increase in 1,3-PDO production and regulation of the cellular metabolic pathway are feasible by electrode-driven control in cathodic electro-fermentation.

Keywords: 1,3-Propanediol; Electrode-driven conversion; Metabolic shift; Bioelectrochemical system; Electro-fermentation

1. Introduction

Electro-fermentation (EF) has been highlighted as a novel bioconversion strategy for the production of value-added chemicals and metabolites[1-4]. The interaction between microbe and a carbon electrode has been reported to alter the microbial intracellular redox balance, shifting the conversion process towards a more reduced or oxidized state [5, 6]. Previous studies have shown that electrode-based regulation triggered a change in the metabolic (carbon) fluxes, and concurrently produced more reduced/oxidized metabolites, such as 3-hydroxypropionic acid, L-lysine, and acetoin[7-13]. Electro-fermentation provides a potential platform to further improve the titer and yield, particularly for targeted oxidized/reduced products in biochemical reactions, which are difficult to achieve through conventional fermentation[1, 4].

1,3-propanediol (1,3-PDO) is an important C3 platform precursor for further chemical synthesis, including the production of polytrimethylene terephthalate. Therefore, the development of 1,3-PDO bio-production from glycerol has been examined previously [14, 15]. Biological glycerol conversion to 1,3-PDO consists of two consecutive reactions: glycerol to 3-hydroxypropionaldehyde (3-HPA) by glycerol dehydratase with coenzyme B_{12} as a cofactor, and 3-HPA to 1,3-PDO by 1,3-propanediol oxidoreductase with a reducing equivalent in the form of NADH [16]. Two moles of additional reducing equivalents are necessary for glycerol-based 1,3-PDO production:

$$\text{Glycerol } (C_3O_3H_8) + 3H_2O \rightarrow 3CO_2 + 14H^+ + 14e^- \quad (1)$$

$$\text{1,3-PDO } (C_3O_2H_8) + 4H_2O \rightarrow 3CO_2 + 16H^+ + 16e^- \quad (2)$$

$$\text{Glycerol } (C_3O_3H_8) + 2H^+ + 2e^- \rightarrow \text{1,3-PDO } (C_3O_2H_8) + H_2O \quad (3)$$

To resolve the electron imbalance between the substrate (glycerol) and product (1,3-PDO), and further increase the level of 1,3-PDO productivity, an appropriate pathway for providing necessary reducing equivalents is essential. Previous studies reported that the activation of byproduct-formation pathways, such as ethanol, 3-hydroxypropionic acid, and 2,3-butanediol, brought additional NADH synthesis and increased 1,3-PDO production [17-20].

Naturally, some facultative anaerobes, such as *Klebsiella*, *Citrobacter*, and *Lactobacillus* species, have indigenous 1,3-PDO producing pathways [14, 21, 22]. *Klebsiella pneumoniae* is one of the best candidates for 1,3-PDO bioproduction, because it possesses crucial active enzymes for the glycerol reductive pathways, natural coenzyme B_{12} synthesis, and a well-developed glycerol uptake module [16]. Among the *K. pneumoniae* strains, *K. pneumoniae* L17 has the ability to exchange respiratory electrons with the electrode [13]. Previous studies have reported that the application of an electrical potential through a carbon electrode in a bioelectrochemical system induced a change in the metabolic flux and gene expression of L17 [12, 13]. Such anodic EF increased the productivity of 3-HP 1.8 fold using a +0.5 V (vs. Ag/AgCl) polarized electrode in a bioelectrochemical system [10].

This study evaluated an electrode-based electron supply for glycerol conversion to 1,3-PDO using *Klebsiella pneumoniae* L17. The current input through the electrode is believed to alter the level of 1,3-PDO production from glycerol compared to the control with a non-polarized electrode. Quantitative flux and transcriptional analyses were performed to determine if the electrode-based electron transference shifts the metabolic state to a more reduced circumstance in glycerol conversion. To enhance electron transfer between the bacteria and electrode, three different electron shuttles were examined: 2-hydroxy-1,4-

napthoquinone, neutral red, and hydroquinone. The recombinant *K. pneumoniae* L17 overexpressing DhaB and DhaT in the glycerol reductive pathway shows that the electrochemical interaction can be corroborated by the appropriate strain development. This is the first *K. pneumoniae* study to examine glycerol conversion to 1,3-PDO by providing a reducing equivalent in a bioelectrochemical system, and simultaneously identifying the change in metabolic flux induced by electrode-driven bioconversion.

2. Materials and methods

2.1. Strains and culture media

Klebsiella pneumoniae L17 (hereinafter L17) was purchased from CCTCC (China Center for Type Culture Collection) and stored at - 80 °C prior to inoculation. Table S1 lists the recombinant L17 and plasmids used in this study. Two plasmids harboring glycerol dehydratase (dhaB) or 1,3-propanediol oxidoreductase (dhaT) were synthesized in the pDK7 or pCU19 vector, respectively [23]. The transformations of each plasmid in L17 were performed using the method reported elsewhere [10]. The modified M9 media with the following composition were used after sterilization by autoclaving or filter-sterilizing: 1 g/L NaCl, 1 g/L NH_4Cl, 0.25 g/L $MgSO_4 \cdot 7H_2O$, 0.5 g/L yeast extract, 150 mM glycerol, 100 mM potassium phosphate (pH = 8.0), 1.25 ml vitamin solution (10x) [13], and 10 ml of trace element solution (1.25x) [13]. The medium was adjusted to pH 7.8 using 10 % HCl and 5 N NaOH solutions. Different concentrations (10 and 100 μM in the final) of electron shuttles (2-hydroxy-1,4-naphthoquinone, HNQ; neutral red, NR; hydroquinone, HQ) were filter-sterilized and added to the cathodic chamber of the bioelectrochemical system.

2.2. Bioelectrochemical system (BES) operation

A H-type two-chamber BES reactor was used as described elsewhere[13]. Both the anode and cathode chambers (310 ml each) were connected with a glass tube bridge and a proton exchange membrane (PEM, Nafion 117, Dupont, USA). Carbon cloth (2.5 cm × 5 cm, Nara Cell-Tech Co., Korea) was used as the anode and cathode electrodes. The Ag/AgCl reference electrode was placed in the cathode chambers. The BES reactor was prewashed completely with 10 % HCl and 5 N NaOH solutions and sterilized in an autoclave (121 °C, 15 min). After sterilization, the cathode chamber was filled with the modified M9 media, while in the anode chamber, 50 mM of ferrous sulfate heptahydrate in 100 mM of potassium phosphate buffer (pH = 8.0) was added (the working volume of both chambers was 250 ml). Before starting the experiments, *K. pneumoniae* L17 was pre-cultured overnight in LB medium, followed by 12 hours of activation in M9 medium. The cathode chamber was inoculated with the pre-cultured L17 (initial OD_{600} = 0.07). Ampicillin was added to the anode and cathode chamber to prevent contamination (100 μM). The BES fermentation media for the recombinant strain culture contained 0.1 mM of IPTG and 25 μM of kanamycin and/or chloramphenicol instead of ampicillin.

Both BES and non-BES (control without externally poised potential) reactors were placed in an incubator (30 °C) on a magnetic stirrer plate (100 rpm). Both anode and cathode chambers were purged continuously with nitrogen gas (99.9 %) to maintain anoxic conditions during the experiment. Chronoamperometry (-0.9 V vs. Ag/AgCl) was performed using a potentiostat (WBCS3000Lee32, WonA Tech, Korea) with an externally poised potential applied continuously to the cathode electrode.

2. 3. Analyses

Samples for the analysis of cell growth, pH, and metabolite concentrations were

taken periodically from the cathode chamber at 0, 6, 12, 24, and 36 h. To analyze the metabolite concentration, the liquid samples were centrifuged (5,000 rpm for 10 min) and filtered using a syringe filter (0.22 μm, Nylon membrane, Whatman, UK). The filtered samples were analyzed by high performance liquid chromatography (HPLC, HP 1160 series, Agilent Technologies, USA) using an Aminex HPX-87H column (300 × 7.8 mm, Bio-Rad, USA) at 65 °C. H_2SO_4 buffer (2.5 mM) was used as the mobile phase (flow rate = 0.5 ml/s), and a refractive index (RI) and photodiode array (PDA) detector were used.

2. 4. Metabolic flux model and analysis

The metabolic network model of glycerol conversion in BES was constructed for *in silico* metabolic flux analysis (MFA), as shown in Table S2 in the Supplementary information. The electron uptake pathways by electron transfer from the electrode were added to the flux model according to the following equation:

$$2\ \text{electron-ex} + Q + 2H^+ \rightarrow QH_2 \qquad (4)$$

Maximization of the cell growth or 1,3-PDO production pathways were the objective functions for the simulation in BESs and non-BESs. Linear optimization using the MetaFluxNet program was implemented to solve the metabolic flux equations [13, 24] .

The expression of essential enzymes for glycerol conversion was investigated by RT-PCR, as reported elsewhere[12]. mRNA extraction was performed using a total RNA isolation kit (Macherey-Nagel, Germany); reverse transcription for cDNA synthesis was conducted using a RevertAid First Strand cDNA synthesis kit (ThermoFisher, USA). The SYBR green method was used for quantitative real-time PCR on a Step One Real Time PCR system (Applied Biosystems, USA). The forward and reverse primers are described

169 elsewhere[12]. All experiments were conducted in quadruplicate.

170

171 ## 3. Results and discussion

172 ### *3.1. Current consumption in BESs with different mediators*

173 Fig 1 shows the current consumption profiles under -0.9V vs. Ag/AgCl during
174 cathodic glycerol conversion. The effects of different electron shuttles (NR and HNQ) with
175 low (10 μM) and high (100 μM) concentrations were compared in the BESs. With the low
176 concentration of electron shuttles, the current consumptions were stabilized at approximately
177 −20, −30, and −110 μA in BES without a mediator (i.e. control) and with HNQ and NR,
178 respectively (hereinafter called BES, BES-HNQ-10, and BES-NR-10) after 12 hours. In
179 contrast, relatively higher current consumption was observed at −100 and −200 μA in BESs
180 with higher concentrations of HNQ and NR (each 100 μM), respectively (hereinafter called
181 BES-HNQ-100 and BES-NR-100). Electron transfer from the electrode was estimated to be
182 0.02, 0.05, and 0.11 mmol based on the Faraday constant (96,485 C/mole of e^-) in BES, BES-
183 HNQ-10, and BES-NR-10, respectively, whereas they were much higher in BES-HNQ-100
184 (0.11 mmol) and BES-NR-100 (0.23 mmol).

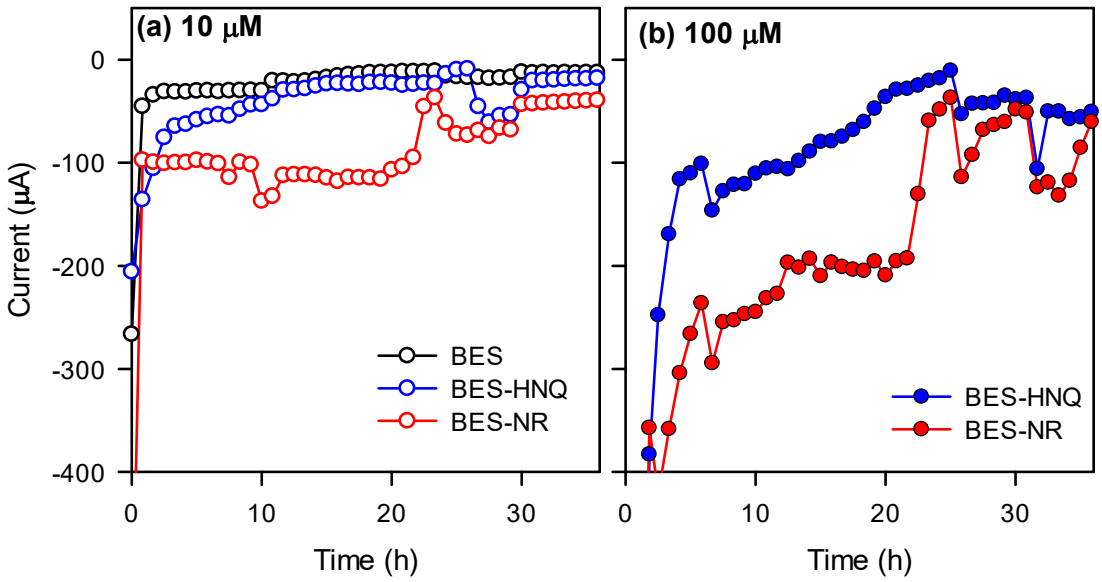

Fig 1. Current generation profiles of BESs with (a) 10 μM and (b) 100 μM of each electron shuttle (HNQ: 2-hydroxy-1,4-naphthoquinone; NR: neutral red)

K. pneumoniae L17 is an exoelectrogen that can transfer/excrete its respiratory electron to the electrode using mainly an indirect electron transfer module via electrochemically active shuttle molecules[10, 12, 13]. This shuttle-based electron transfer was reported to induce a change in the intracellular redox balance and consequently a metabolic shift [12, 13]. Under anodic glycerol electro-fermentation conditions, L17 produced 80% higher 3-hydroxypropinate, while the respiratory electrons were discharged to the anode [10]. On the other hand, 1,3-PDO production from glycerol is a representative reductive bioconversion; the productivity of 1,3-PDO is expected to increase when the reducing equivalent is provided from the electrode by the negatively poised potential on the cathode electrode. According to a previous study, mediator-based electron uptake from the electrode to the inner membrane quinone species could be possible in heterotrophic bacteria of *K. pneumoniae* species when the appropriate redox electron shuttle was provided [25]. Although the mechanism of an increased intracellular redox level by the reduced quinone species is unclear, it is

hypothesized that the reduced quinol species not only block NADH oxidation by the indigenous respiratory system, but also prompt NAD^+ reduction via the cellular NADH dehydrogenases under these cathodic EF conditions [25].

The three electron mediators, 2-hydroxy-1,4-naphtoquinone (HNQ, E^o = -0.6 V vs. SHE), neutral red (NR, E^o = -0.5 V vs. SHE), and hydroquinone (HQ, E^o = -0.7 V vs. SHE), were compared in BES under -0.9V vs. Ag/AgCl (Fig 1). Although electron transfer from the bacteria to the electrode was reported to be facilitated by HNQ in an anodic EF in a previous study[13], the significantly lower electron consumption in cathodic EF (i.e. reverse direction of electron transfer from anodic EF) in Fig 1, suggests that HNQ is less efficient than NR for intracellular electron transfer. In contrast, NR has been used extensively as an electron shuttle in exoelectrogens, which interact with menaquinone in the inner membrane of *E. coli* during electro-fermentation[25]. In this study, the significantly enhanced current consumption was obtained from the NR implemented cathodic EF. HQ has a relatively low molecular weight (MW 110.11) compared to the other two shuttles (HNQ, MW 174.15; NR, MW 288.78), and is expected to have advantages for cellular membrane penetration. On the other hand, no apparent cell growth and glycerol consumption were identified under both BES and non-BES conditions with HQ, probably due to the toxicity of hydroquinone (See Supplementary Information Fig. S4).

3.2. Glycerol consumption and 1,3-PDO production in BESs and non-BESs

Fig 2 and Table 1 present the glycerol uptake and simultaneous 1,3-PDO and ethanol production. Most of the glycerol was consumed in the non-BES system within 12 hours, whereas more than half of the glycerol remained in most of the BESs. The input current

appeared to decrease glycerol consumption, probably due to the more reduced redox circumstance induced by the negatively poised potential. The bacterial growth profiles of different conditions showed a similar trend to glycerol consumption (Fig S2). The growth of non-BES reached the stationary phase within 12 hours, whereas it was obtained at approximately 24 hours in BES. With NR, cell growth was initially retarded, but the final cell concentration was slightly higher than that under the other conditions (Fig S2c). These results show that additional electron transfer to bacteria may decrease the glycerol uptake and consequently the cell growth rate in a cathodic EF.

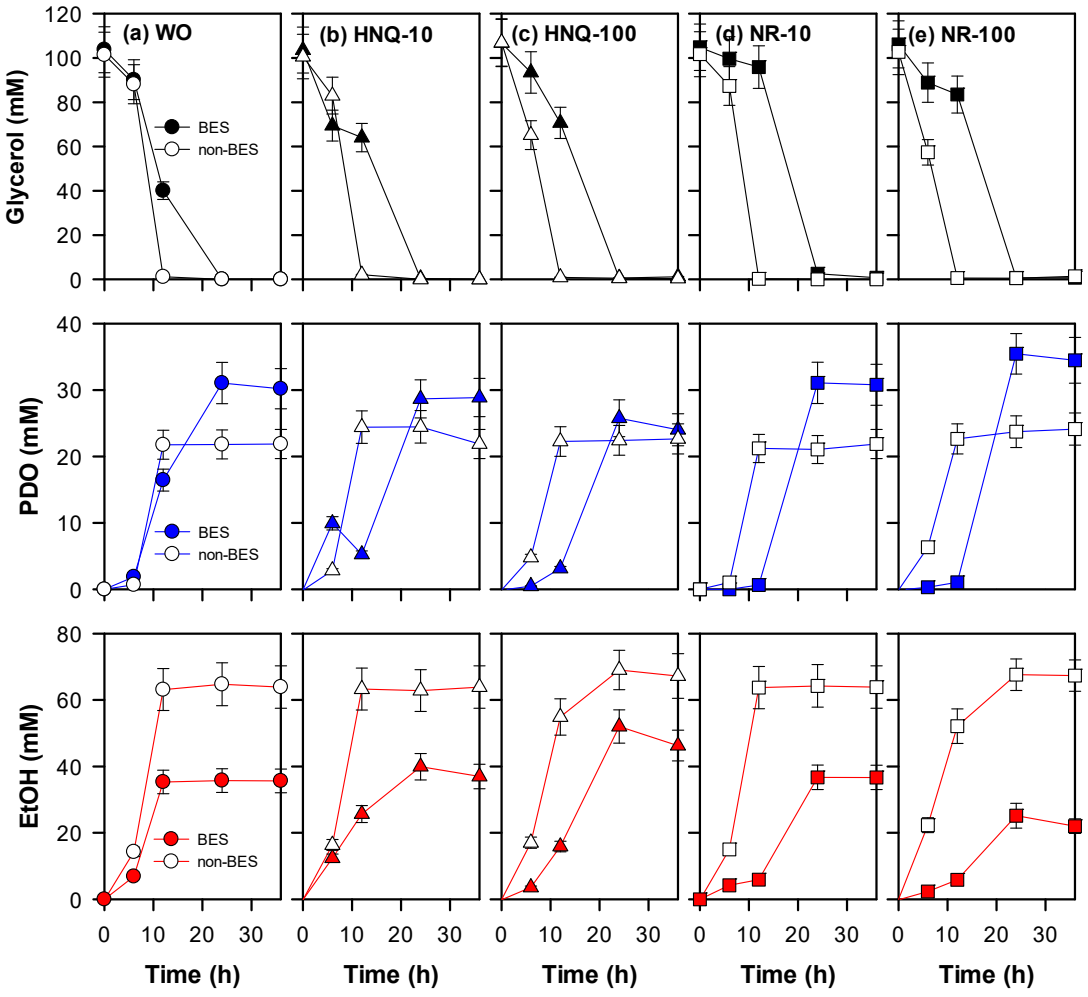

Fig 2. Metabolite profiles (black-glycerol, blue-1,3-PDO, red-ethanol) in BES and non-BES (a) without a mediator, (b) with 10 μM HNQ, (c) with 100 μM NR, (d) with 10 μM

NR, and (e) with 100 μM NR. The closed symbols indicate BES while the open symbols represent non-BES operation.

10.1002/cssc.201902928

238

239 Table 1. Carbon recovery, glycerol consumption, and metabolite production of KpL17 in BESs and non-BESs

	Glycerol consumption (mM)	DCW (g/L)	PDO (mM)	Ethanol (mM)	3-HP (mM)	Lactate (mM)	Acetate (mM)	Succinate (mM)	Carbon recovery (%)
Without mediator									
BES	103.7 ± 3.2	0.7 ± 0.1	31.1 ± 3.0	35.7 ± 3.7	11.4 ± 0.9	5.6 ± 0.9	5.9 ± 0.5	4.1 ± 1.3	94.3
non-BES	101.5 ± 7.1	0.8 ± 0.1	21.8 ± 3.2	64.7 ± 6.5	5.4 ± 0.4	2.1 ± 0.3	3.9 ± 0.3	4.3 ± 1.4	104.6
HNQ-10μM									
BES	103.6 ± 5.6	0.6 ± 0.0	28.7 ± 2.1	39.9 ± 5.0	8.7 ± 0.7	5.6 ± 0.9	6.9 ± 0.5	4.4 ± 1.4	95.5
non-BES	100.7 ± 6.6	0.7 ± 0.1	24.5 ± 2.1	62.8 ± 6.0	6.7 ± 0.5	3.0 ± 0.5	4.9 ± 0.4	2.1 ± 0.7	107.8
HNQ-100μM									
BES	106.2 ± 7.4	0.8 ± 0.1	25.9 ± 2.7	52.0 ± 5.0	11.9 ± 0.8	1.8 ± 0.1	4.7 ± 0.3	4.1 ± 0.3	90.5
non-BES	106.5 ± 7.5	0.8 ± 0.1	22.4 ± 2.2	69.0 ± 5.9	7.2 ± 0.5	6.4 ± 0.5	5.2 ± 0.4	2.6 ± 0.2	102.6
NR-10μM									
BES	104.1 ± 8.0	0.8 ± 0.1	31.1 ± 3.0	36.7 ± 3.1	10.1 ± 0.8	3.9 ± 0.6	4.8 ± 0.4	4.3 ± 1.4	93.2
non-BES	101.7 ± 7.0	0.8 ± 0.1	21.1 ± 2.1	64.2 ± 6.2	5.2 ± 0.4	1.5 ± 0.2	4.4 ± 0.3	4.5 ± 1.4	103.5
NR-100μM									
BES	105.5 ± 7.4	0.8 ± 0.1	35.5 ± 3.1	25.1 ± 3.7	13.5 ± 0.9	3.5 ± 0.2	5.6 ± 0.4	2.4 ± 0.2	91.4
non-BES	102.1 ± 7.2	0.8 ± 0.1	23.7 ± 2.4	67.6 ± 4.8	6.6 ± 0.5	6.0 ± 0.4	5.7 ± 0.4	2.1 ± 0.1	105.5

240

241

The glycerol fermentation pathway of *K. pneumoniae* L17 is well programmed for the production of reduced metabolites, such as 1,3-PDO and ethanol, under anaerobic conditions. 1,3-PDO conversion was relatively higher in BESs (31.1 ± 3.0, 28.7 ± 2.1 and 31.1 ± 3.0 mM in BES, BES-HNQ-10 and BES-NR-10, respectively) than in non-BESs (21.8 ± 3.2, 24.5 ± 2.1 and 21.1 ± 2.1 mM in non-BES, non-BES-HNQ-10 and non-NR-10, respectively). In contrast, significantly lower ethanol production was obtained in BESs (35.7 ± 3.7, 39.9 ± 4.0 and 36.7 ± 3.1 mM in BES, BES-HNQ-10 and BES-NR-10, respectively) than those in non-BESs (64.7 ± 6.5, 62.8 ± 6.0 and 64.2 ± 6.2 mM in non-BES, non-BES-HNQ-10 and non-BES-NR-10, respectively).

The effects of the addition of electron shuttles were obscure with 10 μM, probably due to the low concentration. At higher concentrations (100 μM), however, metabolite production was different (Fig 2c & e). Interestingly, 1,3-PDO production of BES-HNQ-100 (25.9 ± 2.7 mM) was lower than that of BES-HNQ-10 (28.7 ± 2.1 mM). In contrast, the use of NR increased the level of 1,3-PDO production (35.5 ± 3.1 mM of BES-NR-100) significantly compared to BES-NR-10 (31.1 ± 3.0 mM), non-BES-NR-10 (21.1 ± 2.2 mM), and non-BES-NR-100 (23.7 ± 2.4 mM). Ethanol production was higher in BES-HNQ-100 (52.0 ± 5.0 mM) compared to BES-HNQ-10 (39.9 ± 4.0 mM), but a significant decrease in ethanol production was observed in BES-NR-100 (25.1 ± 3.7 mM) compared to BES-NR-10 (36.7 ± 3.1 mM).

Both 1,3-PDO and ethanol are reduced metabolites, which are synthesized by NADH-dependent aldehyde reductases (acetaldehyde reductase and 1,3-propanediol oxidoreductase for ethanol and 1,3-PDO conversion, respectively). On the other hand, the net NADH balances for 1,3-PDO and ethanol conversions are -1 and 0, respectively, based

on the stoichiometric calculation of the glycerol metabolic fluxes (all pyruvate is believed to be converted to acetyl-CoA by pyruvate formate lyase). Therefore, the 1,3-PDO/ethanol ratio can reflect the intracellular redox balance; a higher ratio indicates a more reduced condition. The 1,3-PDO/ethanol ratios from non-BESs were estimated to be 0.32 - 0.39. On the other hand, a significant increase in the ratio was identified in BES without a mediator (BES, 0.87). Although the BES-NR-10 (0.82) was similar to the BES without a mediator, the clear increase in 1,3-PDO/ethanol ratio (1.41) indicates that the intracellular redox state was shifted to a more reduced state when an appropriate shuttle concentration was provided (BES-NR-100). In contrast, the addition of HNQ and the poised potential appeared to have a negative effect on 1,3-PDO production, as illustrated by the decrease in 1,3-PDO/ethanol ratio (0.72 and 0.50 with BES-HNQ-10 and BES-HNQ-100, respectively).

Cathodic EF also produced several acidic byproducts from glycerol (Fig S3). No significant differences in acetate, succinate, and lactate were identified between BES and non-BES. Only 3-HP production was increased under BES conditions (11.4 ± 0.9, 8.7 ± 0.7, 10.1 ± 0.8, 11.9 ± 0.8 and 13.5 ± 0.9 in BES, BES-HNQ-10, BES-NR-10, BES-HNQ-100, and BES-NR-100, respectively) compared to non-BES conditions (5.4 ± 0.4, 6.7 ± 0.5, 5.2 ± 0.4, 7.2 ± 0.5 and 6.6 ± 0.5; non-BES, non-BES-HNQ-10, non-BES-NR-10, non-BES-HNQ-100, and non-BES-NR-100, respectively)

3.3. In silico metabolic flux analysis

The accumulation of metabolites provides information on the metabolic flux during glycerol fermentation in both BES and non-BES. This metabolic history can be interpreted by stoichiometric metabolic flux analysis (MFA) to understand the overall metabolic and

carbon flux. In particular, the identification of a balance between the oxidative and reductive pathway is crucial not only to examine the bacterial metabolism, but also to estimate the productivity of 1,3-PDO in glycerol conversion, and provide a further strategy for an improvement of yield and titer. Fig 3 shows the results of MFA under BES and non-BES conditions. Non-BES could be considered for conventional anaerobic glycerol fermentation because the electrode does not act as an electron acceptor or donor under open circuit conditions. The ratios of glycerol oxidative to reductive pathway were estimated to be approximately 70:30 under non-BES conditions (73:27, 69:31, 74:26, 72:28, and 72:28 in non-BES, non-BES-HNQ-10, non-BES-NR-10, non-BES-HNQ-100, and non-BES-NR-100, respectively). In contrast, relatively higher ratios of reductive pathways were obtained under BES conditions (59:41, 64:36. 61:39, 60:40, and 54:46 in BES, BES-HNQ-10, BES-NR-10, BES-HNQ-100, and BES-NR-100, respectively).

10.1002/cssc.201902928

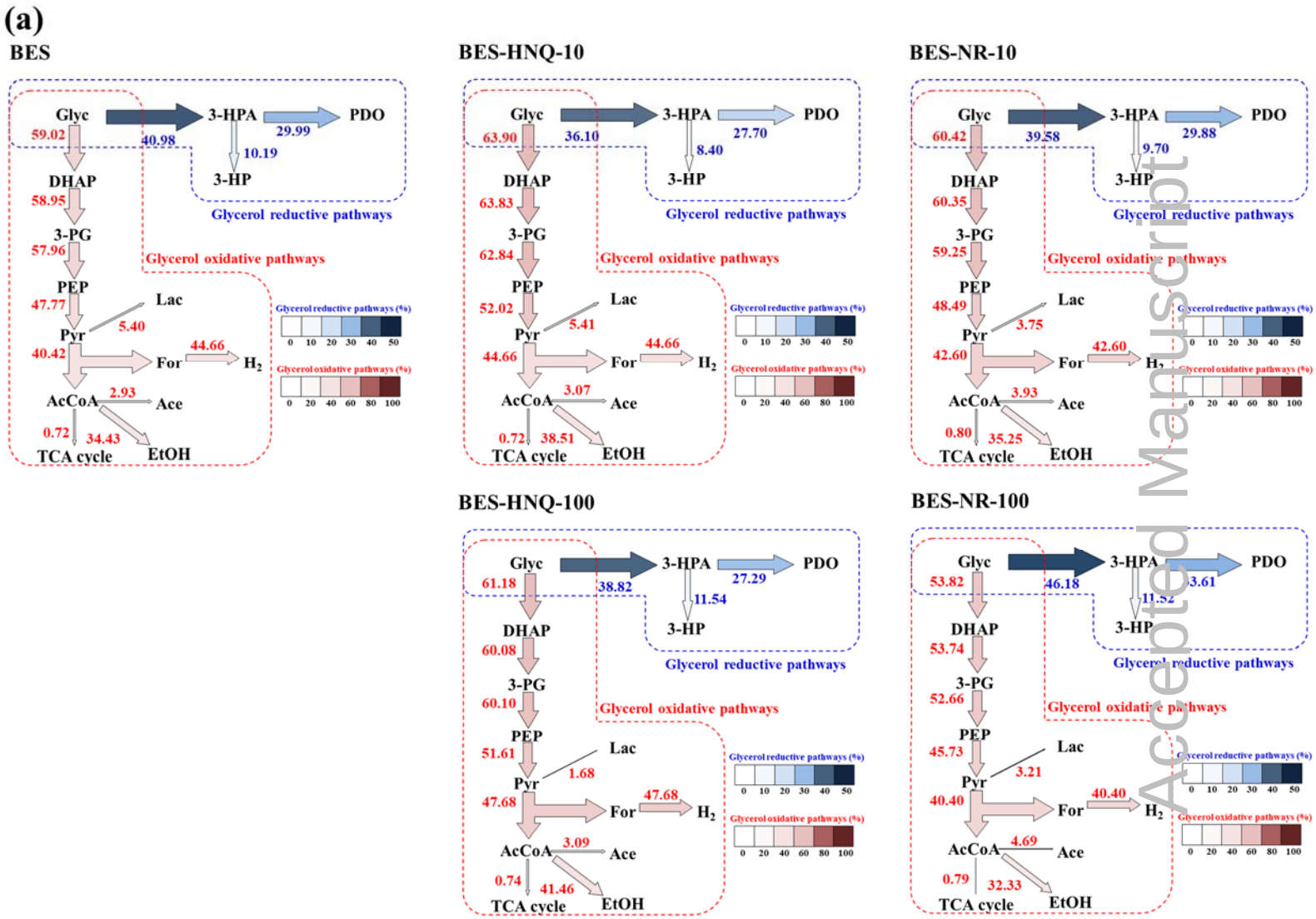

300

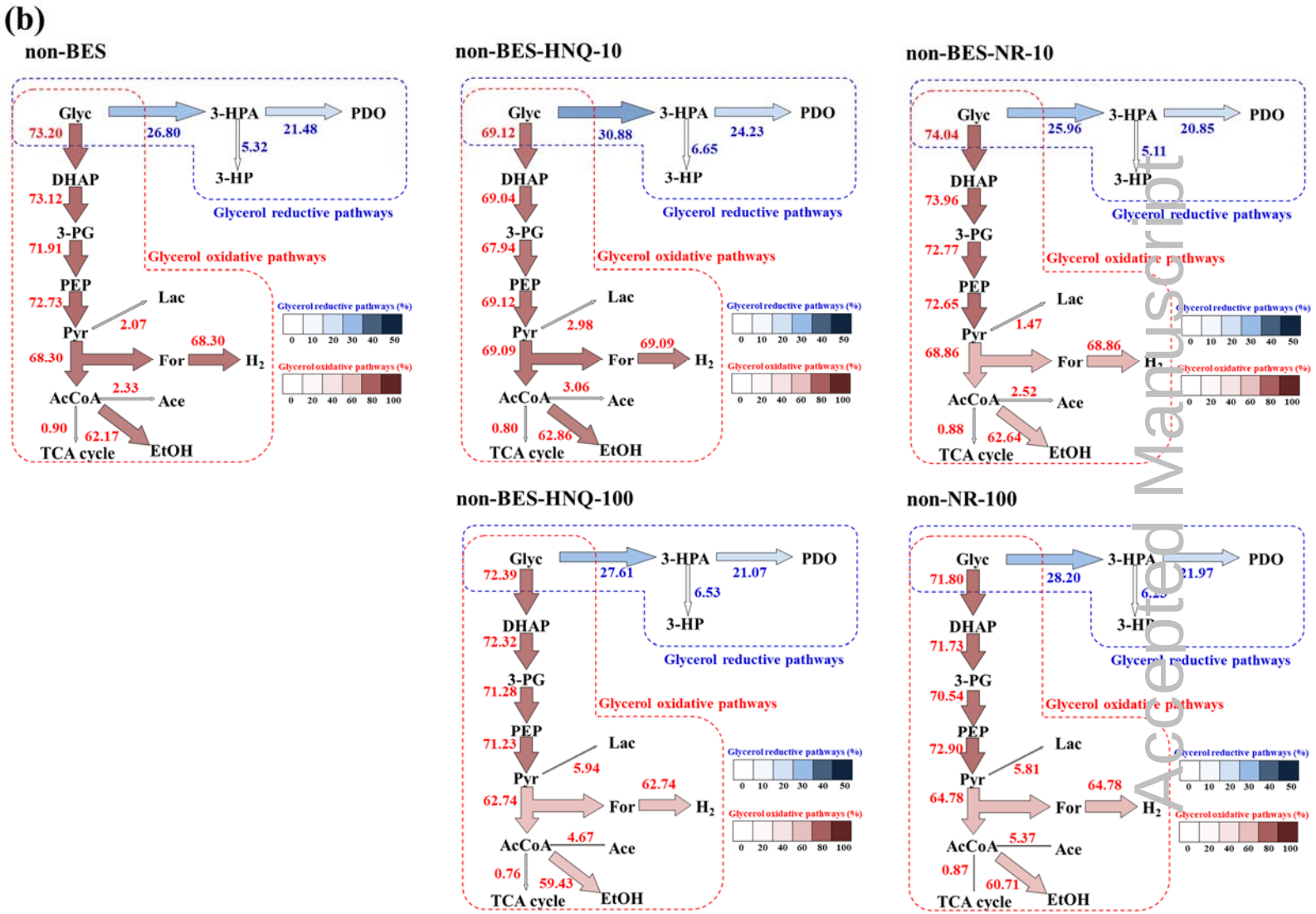

Fig 3. *In silico* metabolic flux balance analysis of BESs (a) and non-BESs (b) with and without electron mediators

Several other metabolites (ethanol, acetate, 3-HP, and succinate) as well as 1,3-PDO were also produced during anaerobic glycerol fermentation. Among them, the 1,3-PDO is the only NADH-consuming product in terms of the net balance. In the metabolic flux analysis of L17 under anaerobic circumstances (including non-BES in this study), the glycerol oxidative to reductive pathway might be programmed naturally as 70:30 based on the estimated 1,3-PDO/ethanol ratio of 0.35, as described above. The externally poised potential shifted the ratio to a more reductive pathway of 60:40 with a higher 1,3-PDO/ethanol ratio of 0.87 under BES conditions. On the other hand, 6.1 mmol of electron recovery is required for 11.8 mM of 1,3-PDO production in BES-HNQ-100 (estimated by NADH consumption) compared to that under non-BES conditions. Nevertheless, it was estimated that only 0.23 mmol of electrons were actually transferred from the electrode in BES-NR-100 (even under the assumption that all the electrons were transferred to the bacteria and converted to NADH) (Fig. 1), which is significantly lower than the amount of 1,3-PDO produced. In addition, the 'rebalance' of reducing equivalent under BES condition (i.e. additional NAD(P)H from the reduced metabolites production such as ethanol and lactate) may influence 1,3-PDO conversion. A similar electricity-driven metabolic shift was reported in an electroactive heterotroph *Clostridium pasteurianum* for 1,3-PDO production from glycerol[7]. In this study, a small amount of electron uptake induces the NADH-consuming pathways over the stoichiometric contribution of the electrons. These results suggest that a small current uptake might result in a dramatic change in the metabolic flux under the unnatural conditions of cathodic EF for 1,3-PDO production. The triggering effect by the poised potential and current in EF requires further study for engineering applications to enhance the yield and titer of the target products.

3.4. Transcriptional analysis of glycerol conversion under cathodic EF

To determine if the poised potential shifts the transcription of the gene, the expression levels of the three major glycerol assimilating enzymes, glycerol kinase (GlpK), glycerol dehydrogenase (DhaD) and glycerol dehydratase (DhaB), were investigated by RT-PCR (Fig 4). Significantly lower (0.7 fold, dhaD) and higher (4.8 fold, dhaB) expression levels were analyzed from BES than those of non-BES, respectively, whereas the difference in glpK was negligible in both conditions. These results show that the electrode-based reducing equivalent transfer affects the expression of enzymes involved in glycerol conversion, and activates the reductive pathway rather than the oxidative pathway.

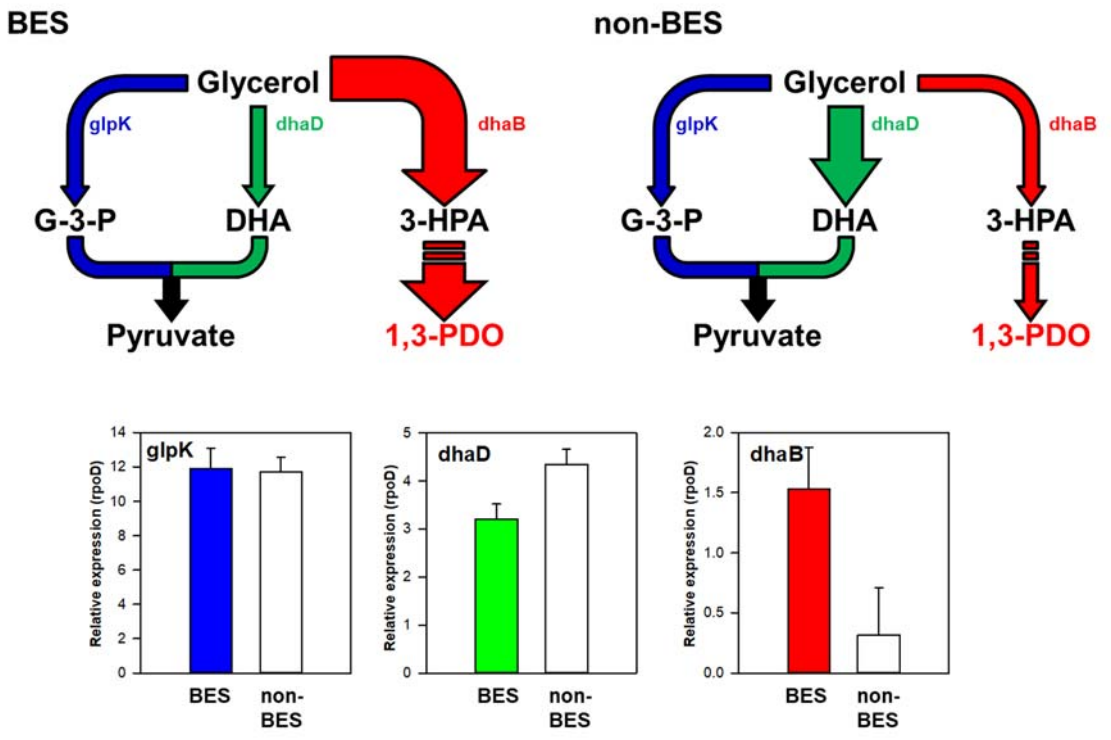

Fig 4. mRNA expression profiles for glycerol-converting enzymes (glpK, dhaD and dhaB). Both BES and non-BES used NR (100 mM) as an electron shuttle

K. pneumoniae has three glycerol utilization pathways: glp and dhaD module for the oxidative pathway, and the reductive pathway via dhaB. Under aerobic conditions, glycerol would be phosphorylated into glycerol-3-phosphate (G-3-P) by glycerol kinase (GlpK). G-3-P is oxidized further by GlpD (glycerol-3-phosphate dehydrogenase) to synthesize dehydroxyactone-phosphate (DHAP) for the central carbon assimilation pathways (see Supplementary Information Fig. S1). Under anaerobic conditions, two different cascade modules and reactions are required for glycerol oxidation or reduction: glycerol to dihydroxyacetone (by DhaD, glycerol dehydrogenase), then to dihydroxyacetone phosphate (by DhaK, dihydroxyacetone kinase). Through both aerobic and anaerobic glycerol oxidation, one DHAP is produced from one mole of glycerol with equivalent NADH production and ATP consumption. In contrast, glycerol reduction is conducted in two steps in the reductive pathway: glycerol to 3-HPA and 3-HPA (by DhaB, glycerol dehydratase) to 1,3-PDO (by DhaT, 1,3-propanediol oxidoreductase). The net reaction of glycerol reduction is as follows:

$$\text{Glycerol} + \text{NADH} \rightarrow \text{1,3-PDO} + \text{NAD}^{+} \quad (5)$$

GlpR regulates the expression of the glp regulon, which consists of glpK and glpD as a repressor [16]. G-3-P has high affinity to GlpR and the formation of G-3-P and GlpR complex then renders less repression of glpK and glpD as well as other glp module enzymes (e.g. glpF). In this study, L17 in both BES and non-BES have much less activity for extracellular electron transfer; GlpD has difficulty in catalyzing G-3-P to DHAP. Therefore, the expression of glpK should not change according to externally provided electrons. On the other oxidative pathway regulator, the dha regulon is controlled by DhaR as an activator [26,

[27]. One subunit of DhaK (DhaKII::ADP) is an activator of DhaR; another subunit of DhaK (DhaKI) is an antagonist for DhaKII. DhaD oxidizes glycerol to DHA using NAD^+ as a cofactor. DHA decreases the DhaKI affinity to bind DhaR. In other words, the availability of NAD^+ can determine not only the level of DHA production by DhaD, but also dha regulon expression by the interruption of DhaKI binding to DhaR. Under BES conditions, additional reducing energy from the electrode might increase the NADH/NAD^+ ratio and decrease the expression of the dha regulon, including DhaD, as shown in Fig 4. Although the transcriptional regulation of dhaB of *K. pneumoniae* has not been identified clearly, the high level of dhaB expression in BES might indicate that one of the bacterial redox regulators (probably not an oxygen sensing regulator), would control dhaB expression under cathodic EF condition [28].

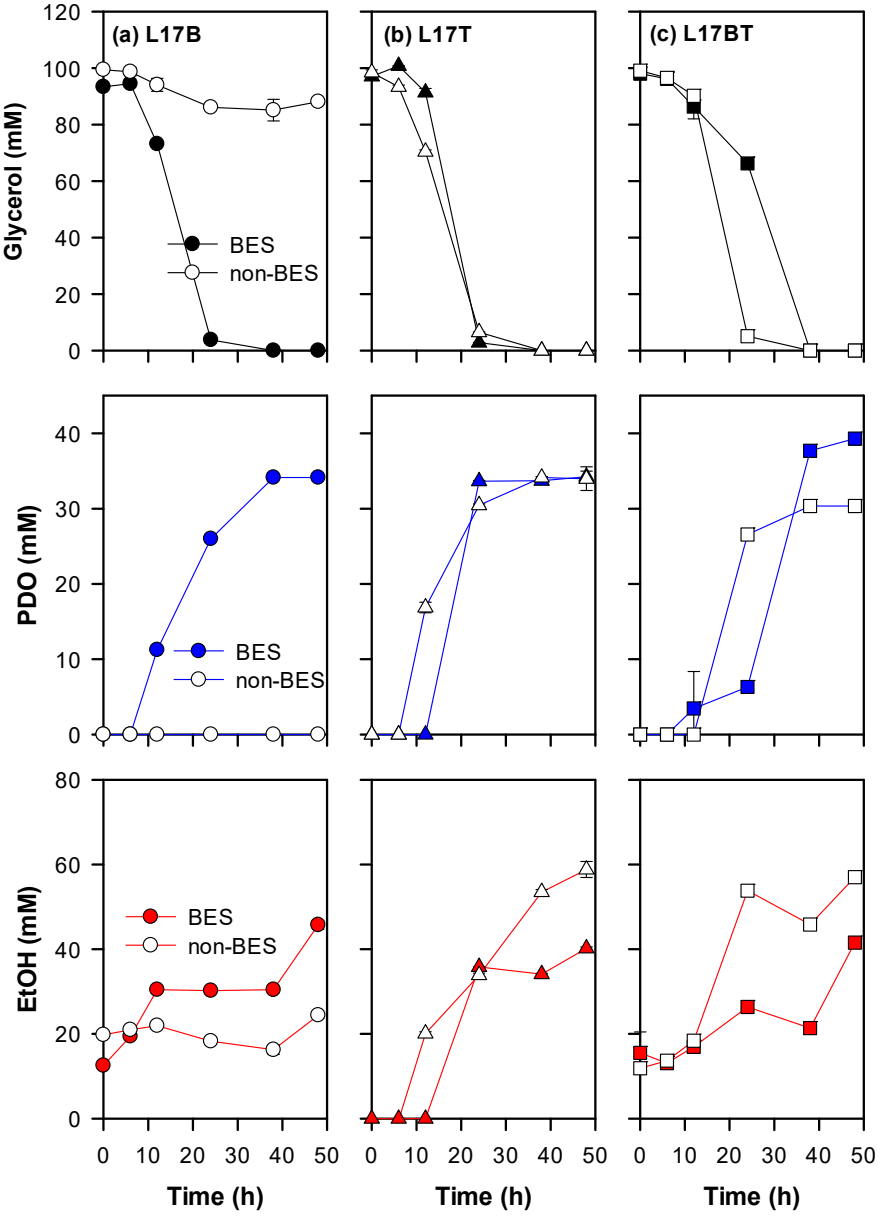

Fig 5. Glycerol, PDO, and EtOH metabolites profiles of BES and non-BES using recombinant L17 strains of L17B (overexpression of DhaB only), L17T (DhaT only) and L17BT (both DhaB and DhaT). The closed symbols indicate BES while the open symbols represent the non-BES operation.

3.5. 1,3-PDO production using recombinant L17

To improve the 1,3-PDO productivity further, the glycerol reductive pathway was overexpressed in L17. Three strains harboring the plasmid for the overexpression of dhaB and/or dhaT were developed: L17B (overexpression of DhaB only), L17T (DhaT only), and L17BT (both DhaB and DhaT) (See Supplementary Information Table S1). L17B showed significantly less glycerol consumption without PDO production under non-BES conditions, whereas the poised potentials enabled the utilization of glycerol and produced 1,3-PDO simultaneously under BES conditions (Fig 5a). The L17T showed similar 1,3-PDO production (34.2 ± 0.8 and 34.0 ± 1.6 mM, respectively) in both BES and non-BES (Fig. 5b). The improvement of 1,3-PDO production was identified in L17BT in BES (39.3 ± 0.8 mM) compared to L17BT in non-BES (30.5 ± 0.5 mM) (Fig. 5c), and wild type L17 in the same BES (35.5 ± 3.1 mM of BES-NR-100) (Fig. 2e).

Generally, glycerol dehydration by DhaB is considered a rate-limiting step for PDO production[27]; hence, the transcription level of DhaB appears to have increased under BES conditions, as shown in Fig. 4. The Lac promoter-based homologous overexpression of DhaB only in the *K. pneumoniae* strain (including L17B results) usually causes the accumulation of the toxic intermediate (3-HPA). Accordingly, glycerol fermentation in non-BES was interrupted significantly, resulting in negligible cell growth [27]. In contrast, the same strain under BES conditions exhibited similar behavior to the wild type and other robust recombinant strains. This suggests that cathodic electron transfer might lead to the expression and/or activation of unknown reductases, which are isoenzymes for DhaT, and concurrently alleviates the accumulation of toxic intermediate under cathodic EF conditions.

Based on these results, intracellular electron transfer from the electrode may function as an activator for the expression of the reductive pathway. Although the

406 overexpression of dhaT increased 1,3-PDO production, regardless of BES and non-BES
407 conditions, as shown in Fig. 5b [29], significantly less ethanol production was also obtained in
408 non-BES. These results suggest that the poised potential efficiently drives the pathway to a
409 more reductive direction in both L17T and L17BT compared to L17B. The simultaneous
410 overexpression of both dhaB and dhaT facilitates L17BT to produce higher 1,3-PDO levels
411 by providing reducing energy from the poised electrode and the homologous expression of
412 essential enzymes for glycerol conversion.
413
414 *3.4. Implications*

415 Glycerol is a relatively reduced feedstock for bioconversion. Anoxic glycerol
416 utilization generally increases the intracellular NADH/NAD^+ level because two moles of
417 NADH are synthesized to produce one mole of pyruvate. Accordingly, the reductive pathway
418 is activated in glycerol fermentation (e.g. for the production of 1,3-PDO). The natural
419 glycerol metabolic flux of *Klebsiella* sp. might be well programmed for the maintenance of
420 redox homeostasis by auxiliary reduction/oxidation pathways. Nevertheless, providing an
421 additional electrode-based reducing equivalent, which was attempted in this study, alters the
422 homeostasis to drive a more reduced circumstance, and then activates the reductive modules
423 of glycerol conversion simultaneously.

424 Electro-fermentation allows electrode-based microbial redox control for
425 bioconversion. Recently, the application of EF to various bioprocesses has been highlighted
426 because the electrode acts as an electron donor/acceptor that can be regulated by electrical
427 energy. EF is expected to replace the use of conventional oxidizing/reducing reagents, which
428 not only increases the operating cost, but also accumulates undesirable toxic byproducts. In

particular, the electricity from future energy infrastructure, including renewable energy systems, can be utilized in the bioprocess through an EF platform. In-situ monitoring and control by an electrode-based bioprocess are other advantages with the efficient management of the product yield and titer. On the other hand, one of the main challenges of EF is that most industrially available strains (e.g. *E. coli*) do not have sufficient electro-chemical activity; hence, the intra- and extra- cellular electron transfer rate in those strains is limited. This drawback might be overcome to some extent using redox shuttles and electrochemically reversible reagents, such as neutral red and designed shuttle molecules.

These results also suggest that the small electron input shifts the entire metabolic fluxes and simultaneously produces higher yields of 1,3-PDO in the cathodic EF of glycerol. The coulombic efficiencies of electro-fermentation are generally low (1 to 38%) using fermentable substrates, such as glycerol, glucose, sucrose and lactose [1].This result can be compared with another representative cathodic conversion of CO_2, microbial electrosynthesis, with 70-100 % coulombic efficiency in BES, which suggests that most of the electrons transferred from the cathode are delivered to CO_2 reduction by bacteria [30]. The significant difference in electron recovery is due to the different redox levels of the starting feedstock (glycerol vs. CO_2). In the glycerol EF, electron transfer by the electrode affects the intracellular redox balance, and triggers a rebalance of the metabolic flux by expression/depression of the involved enzymes. This metabolic 'butterfly effect' could be applied to various bioconversions for the reduction/oxidation of feedstock using not only the electro-chemically active strain in EF, but also conventional fermentation using a range of industrially available strains.

4. Conclusion

453 The cathodic electro-fermentation of glycerol to 1,3-PDO was examined with
454 different electron shuttles, HNQ, NR, and HQ using a *Klebsiella pneumoniae* L17. The
455 externally poised potential of - 0.9 V vs. Ag/AgCl clearly increased the level of 1,3-PDO
456 conversion 1.5 fold (6.1 mmol increase) with 100 μM of neutral red compared to the control,
457 even with a small amount of electron transfer (0.23 mmol). Stoichiometric and transcription
458 analyses showed that supplying reducing energy by the electrode shifts the glycerol
459 metabolic flux to the reductive pathway. The recombinant strain of L17 with the homologous
460 overexpression of DhaB and DhaT enzymes enhanced 1,3-PDO production further (39.3 ±
461 0.8 mM) under EF conditions. This suggests that even a small amount of electron transfer
462 can induce an intracellular metabolic shift, leading to a significant improvement in
463 productivity.
464

465 **Acknowledgements**

466 This study was supported by the Mid-Career Researcher Program (NRF-
467 2018R1A2B6005460) and C1 Gas Refinery Programs (NRF-2018M3D3A1A01055756 &
468 NRF-2015M3D3A1A01064929) through the National Research Foundation of Korea (NRF)
469 funded by the Ministry of Science, ICT & Future Planning, Korea.

References

[1] R. Moscoviz, J. Toledo-Alarcón, E. Trably, N. Bernet *Trends in biotechnology*. **2016**, *34*, 856-865.
[2] R. Moscoviz, E. Trably, N. Bernet *Microbial Biotechnology*. **2018**, *11*, 74-83.
[3] K. Rabaey, R. A. Rozendal *Nature Reviews Microbiology*. **2010**, *8*, 706.
[4] A. Schievano, T. P. Sciarria, K. Vanbroekhoven, H. De Wever, S. Puig, S. J. Andersen, K. Rabaey, D. Pant *Trends in biotechnology*. **2016**, *34*, 866-878.
[5] M. Ishikawa, Y. Tanaka, R. Suzuki, K. Kimura, K. Tanaka, K. Kamiya, H. Ito, S. Kato, T. Kamachi, K. Hori *Bioresource Technology*. **2017**, *241*, 1157-1161.
[6] V. J. Watson, B. E. Logan *Biotechnology & Bioengineering*. **2010**, *105*, 489-498.
[7] O. Choi, T. Kim, H. M. Woo, Y. Um *Scientific Reports*. **2014**, *4*, 6961.
[8] T. Bursac, J. A. Gralnick, J. Gescher *Biotechnology and Bioengineering*. **2017**, *114*, 1283-1289.
[9] A. H. Förster, S. Beblawy, F. Golitsch, J. Gescher *Biotechnology for Biofuels*. **2017**, *10*, 65.
[10] C. Kim, M. Y. Kim, I. Michie, B.-H. Jeon, G. C. Premier, S. Park, J. R. Kim *biotechnology for Biofuels*. **2017**, *10*, 199.
[11] I. Vassilev, G. Gießelmann, S. K. Schwechheimer, C. Wittmann, B. Virdis, J. O. Krömer *Biotechnology and Bioengineering*. **2018**, *115*, 1499-1508.
[12] M. Y. Kim, C. Kim, S. K. Ainala, H. Bae, B.-H. Jeon, S. Park, J. R. Kim *Bioelectrochemistry*. **2019**, *125*, 1-7.
[13] C. Kim, S. K. Ainala, Y.-K. Oh, B.-H. Jeon, S. Park, J. R. Kim *Biotechnology & Bioprocess Engineering*. **2016**, *21*, 250-260.
[14] C. Lee, M. Aroua, W. Daud, P. Cognet, Y. Pérès-Lucchese, P. Fabre, O. Reynes, L. Latapie *Renewable & Sustainable Energy Reviews*. **2015**, *42*, 963-972.
[15] S. Lama, E. Seol, S. Park *Bioresource Technology*. **2017**, *245*, 1542-1550.
[16] V. Kumar, S. Park *Biotechnology Advances*. **2018**, *36*, 150-167.
[17] V. Kumar, M. Sankaranarayanan, M. Durgapal, S. Zhou, Y. Ko, S. Ashok, R. Sarkar, S. Park *Bioresource Technology*. **2013**, *135*, 555-563.
[18] V. Kumar, M. Sankaranarayanan, K.-e. Jae, M. Durgapal, S. Ashok, Y. Ko, R. Sarkar, S. Park *Applied Microbiology & Biotechnology*. **2012**, *96*, 373-383.
[19] S. Ashok, S. M. Raj, C. Rathnasingh, S. Park *Applied Microbiology & Biotechnology*. **2011**, *90*, 1253-1265.
[20] M. Metsoviti, K. Paraskevaidi, A. Koutinas, A.-P. Zeng, S. Papanikolaou *Process Biochemistry*. **2012**, *47*, 1872-1882.
[21] R. Saxena, P. Anand, S. Saran, J. Isar *Biotechnology Advances*. **2009**, *27*, 895-913.
[22] S. K. Ainala, S. Ashok, Y. Ko, S. Park *Applied Microbiology & Biotechnology*. **2013**, *97*, 5001-5011.
[23] Y. Ko, S. Ashok, S. Zhou, V. Kumar, S. Park *Process biochemistry*. **2012**, *47*, 1135-1143.
[24] D.-Y. Lee, H. Yun, S. Park, S. Y. Lee *Bioinformatics*. **2003**, *19*, 2144-2146.
[25] T. D. Harrington, A. Mohamed, V. N. Tran, S. Biria, M. Gargouri, J.-J. Park, D. R. Gang, H. Beyenal *Bioresource Technology*. **2015**, *195*, 57-65.
[26] D. Wei, M. Wang, B. Jiang, J. Shi, J. Hao *Journal of Biotechnology*. **2014**, *177*, 13-19.
[27] P. Zheng, K. Wereath, J. Sun, J. van den Heuvel, A.-P. Zeng *Process Biochemistry*. **2006**, *41*, 2160-2169.
[28] Y. Huang, Z. Li, Q. Ye *Applied Biochemistry & Biotechnology*. **2016**, *178*, 1129-1140.
[29] Z. Chen, H. Liu, D. Liu *Enzyme and Microbial Technology*. **2009**, *45*, 305-309.
[30] C. H. Im, Y. E. Song, B.-H. Jeon, J. R. Kim *Carbon Letters*. **2016**, *20*.